DOE/NASA/1040-78/5
NASA TM-79038

BASELINE PERFORMANCE OF THE GPU 3 STIRLING ENGINE

Lanny G. Thieme and Roy C. Tew, Jr.
National Aeronautics and Space Administration
Lewis Research Center

Work performed for
U. S. DEPARTMENT OF ENERGY
Office of Conservation and Solar Applications
Division of Transportation Energy Conservation

TECHNICAL PAPER presented at the
Highway Vehicle Systems Contractors
Coordination Meeting sponsored by the
U.S. Department of Energy
Dearborn, Michigan, October 17-20, 1978

DOE/NASA/1040-78/5
NASA TM-79038

BASELINE PERFORMANCE OF THE GPU 3 STIRLING ENGINE

Lanny G. Thieme and Roy C. Tew, Jr.
National Aeronautics and Space Administration
Lewis Research Center
Cleveland, Ohio 44135

Prepared for
U. S. DEPARTMENT OF ENERGY
Office of Conservation and Solar Applications
Division of Transportation Energy Conservation
Washington, D. C. 20545
Under Interagency Agreement EC-77-A-31-1040

Highway Vehicle Systems Contractors
Coordination Meeting
sponsored by the U. S. Department of Energy
Dearborn, Michigan, October 17-20, 1978

BASELINE PERFORMANCE OF THE GPU 3 STIRLING ENGINE

by L. G. Thieme and R. C. Tew, Jr.

NASA Lewis Research Center
Cleveland, Ohio 44135

ABSTRACT

The NASA Lewis Research Center has converted a 10 horsepower single-cylinder rhombic-drive Stirling engine to a research configuration to obtain data for validation of Stirling computer simulations. The engine was originally built by General Motors Research Laboratories for the U.S. Army in 1965 as part of a 3 kW engine-generator set, designated the GPU 3 (Ground Power Unit). This report presents test results for a range of heater gas temperatures, mean compression-space pressures, and engine speeds with both helium and hydrogen as the working fluids. Also shown are initial data comparisons with the NASA-Lewis computer simulation predictions.

E-9839

INTRODUCTION

This work was done in support of the U.S. Department of Energy's (DOE) Stirling Engine Highway Vehicle Systems Program. The Lewis Research Center, through Interagency Agreement EC-77-A-31-1040 with DOE, is responsible for project management of this effort under the programmatic direction of the DOE Division of Transportation Energy Conservation.

As part of the NASA Lewis Research Center (LeRC) in-house technology program, a 10 HP single-cylinder rhombic-drive Stirling engine has been obtained and restored to operating condition. The engine was originally built by General Motors Research Laboratories for the Army in 1965 as part of a 3 kW engine-generator set, designated the GPU 3 (Ground Power Unit).

One of the principal objectives of this engine testing is to obtain and publish detailed engine performance data which can be used with the engine dimensions necessary for modeling to develop Stirling simulation techniques. The data will also be used for modification and validation of the NASA LeRC Stirling computer simulation. To obtain this data, the engine was converted to a research configuration. The engine-driven accessories from the original GPU 3 package were removed and extensive instrumentation added.

Baseline tests were then run to map the engine over a range of heater gas temperatures, mean compression-space pressures and engine speeds with both helium and hydrogen as the working fluids. Tests,

however, were limited to the lower power levels due to use of the original alternator and a resistance load bank which were not capable of absorbing the full engine output power.

This report presents selected results from these tests to identify the experimental trends of the data that were taken. Also shown are initial data comparisons with the NASA-LeRC simulation predictions.

Initial results with the engine tested as part of the original GPU 3 package and a description of the original engine components and systems are given in reference 1.

A dynamometer facility is now being prepared which will allow engine mapping at the higher power levels. Motoring tests will also be run to aid in determining the mechanical losses.

GPU 3 PROJECT OBJECTIVES

The GPU 3 Stirling engine test program at the LeRC has the following objectives. The first is to obtain and publish detailed engine performance data. This data along with the engine dimensions necessary for modeling should assist in the development of Stirling simulation techniques.

The second objective is to validate, document, and publish the NASA-LeRC computer model. This model is described in reference 2. Testing to provide the required data will include the following: mapping the engine at various speeds, pressures, and temperatures (heater gas and cooling water inlet), tests with advanced instrumentation for dynamic cycle measurements, and specific parametric tests such as determining the effect of dead volume variation.

Finally, the engine will provide a test bed for evaluation of new system and component concepts from the supporting Stirling engine technology programs.

APPARATUS AND PROCEDURE

GPU 3 Stirling Engine

Figure 1 is a photograph of the GPU 3 (Ground Power Unit) Stirling engine as most recently tested at the NASA-LeRC. The engine was obtained from the U.S. Army Mobility Equipment Research and Development Center (MERDC) at Fort Belvoir, Virginia. A second identical engine was also obtained through loan from the Smithsonian Institution. This second engine so far has been used as a source of spare parts for the Army engine.

Both engines were originally part of identical 3 kW engine-generator sets built by General Motors Research Laboratories in 1965 for the U.S. Army. These units were completely self-contained and capable of operation using a variety of fuels over a broad range of ambient conditions. They were designed for using hydrogen as the working fluid.

The GPU 3 engine is a single-cylinder displacer-type engine with a rhombic drive and sliding rod seals. It is capable of producing a maximum of approximately 10 bhp with hydrogen working fluid at 1000 psi mean compression-space pressure. The piston swept volume is 7.3 in^3.

GPU 3 Test Setup

The test setup for the initial baseline testing of the GPU 3 is shown in figure 2. For these runs, the following changes were made to convert the engine to a research configuration. Where necessary, new parts (power piston, cooler-regenerator cartridges, displacer shaft) were made and others (fuel nozzle) reworked to allow successful operation. All engine-driven accessories were removed with the exception of the oil pump. Air, water, fuel, and working fluid were provided from the facility. Dimensional measurements, flow tests of the heat exchangers, and volume measurements of the working space were completed. The control system of the original GPU 3 unit was replaced with manual controls. Finally, instrumentation was added to allow obtaining an energy balance, engine temperature profiles, working space gas temperatures and dynamic pressures and an attempt to measure indicated work.

The original GPU 3 alternator and a separate resistance load bank were used to absorb the engine output power. The alternator was calibrated to define its efficiency at various speeds and output voltages. Since the original GPU 3 package was designed for a 3 kW output, the alternator was not capable of the maximum output of the engine. Thus, these tests were limited by the method of power absorption. Specifically, the restrictions were maximum alternator current, alternator calibration range, and load bank capacity.

The fuel flow measurement was made with two external tanks. One tank was used to supply fuel during startup and while establishing a data point. The second tank was used while data were being taken. Its weight was recorded before and after each data point to determine the amount of fuel used. The fuel for these tests was No. 1 diesel fuel.

Test Method

Each curve of these tests was run at constant mean compression-space pressure, heater tube gas temperature, and cooling water flow. At each point the load was adjusted to establish the desired speed.

The combustion air flow was set to approximately maintain a constant air-fuel ratio.

The heater tube gas temperature was measured with thermocouple probes installed inside three of the forty heater tubes and spaced circumferentially around the heater head. The maximum reading of these three thermocouples was controlled to the desired temperature by adjusting the fuel flow with a needle valve. The cooling water inlet temperature was not controlled and varied about 10° F over the series of tests.

After each engine start up, a reference point (1300° F heater gas temperature, no load, 3000 rpm) was first established to verify proper engine operation and to allow the engine to reach operating temperatures. Each point was then maintained for 15 minutes after reaching desired conditions with all steady-state data being recorded three times during this period. The fuel flow was determined for this 15 minute interval.

The test matrix range for both the helium and hydrogen runs was as follows: mean compression-space pressure 200-1000 psi, heater tube gas temperature 1100-1300° F, and engine speed 1000 to 3500 rpm.

RESULTS AND DISCUSSION

The curves shown in this report were selected to identify the experimental trends of the data that were taken. All data will be published at a later date.

Figure 3 shows engine output and brake specific fuel consumption (BSFC) vs. engine speed as a function of mean compression-space pressure. The working fluid is helium at a heater tube gas temperature of 1200° F. The engine output was determined by measuring output power of the alternator and dividing this by the alternator efficiency.

The incomplete curves at the higher pressure levels indicate the limiting effect of the alternator and load bank. The alternator output current increased with decreasing speed and eventually reached its maximum allowed value. This point then determined the range of speeds for a given pressure at which the engine could be operated.

For a constant pressure, the engine output and brake thermal efficiency tend to decrease at the higher speeds. This is primarily due to the increasing flow losses through the heat exchangers. At the lower speeds, the conduction losses become a significant percentage of the heat input and cause the efficiency to decrease. Thus, the efficiency tends to maximize (minimum BSFC) at some intermediate speed as shown in the figure.

For a given speed the engine output and efficiency both increase with increasing pressure level. However, the spacing between the curves shows that as the pressure increases, the relative gain in power and particularly, the relative gain in efficiency decrease. This can be attributed in part to the effect of heat transfer limitations at the cold end of the engine. For a fixed speed, the compression space gas temperature increases with pressure. For example, the compression space gas temperature rose from 195° F at 400 psi, 3000 rpm to 247° F at 1000 psi, 3000 rpm. Thus, the Carnot efficiency based on the gas temperatures is less for the higher pressure levels although the heater gas temperature and cooling water inlet temperature remain the same.

A similar set of curves was run at 1300° F heater gas temperature. However, the alternator and load bank limitation would not allow operation at this temperature at the maximum engine pressure of 1000 psi. The 1200° F curves were included in this report as they indicate the highest power of 5.25 hp obtained with helium. The minimum BSFC measured was 0.99 lb/bhp-hr which corresponds to 13.9 percent brake thermal efficiency.

Test data were taken to determine the effect of varying heater tube gas temperature. For a constant mean compression-space pressure, curves were run at heater gas temperatures of 1100, 1200, and 1300° F. Figure 4 shows engine output and BSFC at these temperatures for helium at 400 psi. Similar sets of curves were obtained for helium at 800 psi and hydrogen at 400 psi. The limitation on power absorption due to the alternator and load bank precluded hydrogen operation at the 800 psi pressure level.

Hydrogen results for engine output and BSFC vs. engine speed as a function of mean compression-space pressure are shown in figure 5. The heater gas temperature is 1300° F.

These data were taken over less of a pressure range than were the helium data due to the higher power output with hydrogen at a given pressure. This causes the limiting alternator values to be reached at a lower pressure level.

The maximum engine output with hydrogen was 6.0 hp at 600 psi, 3500 rpm. The minimum BSFC was 0.81 lb/bhp-hr at 400 psi, 2500 rpm. This corresponds to a brake thermal efficiency of 16.9 percent.

Note that the hydrogen power curves are more linear with speed and peak out at a much higher speed than do the corresponding helium curves. This is an indication of the lower flow losses associated with hydrogen compared to helium.

Figure 6 gives two examples of an energy balance on the engine operating with helium. Both points are for a heater gas temperature of 1200° F and an engine speed of 3000 rpm. The first is for an engine output of 1.4 hp at 400 psi mean compression-space pressure while the other is for an engine output of 5.2 hp at 1000 psi.

The bargraphs indicate that more than 97 percent of all heat input was accounted for at these two points. The range of input energy accounted for in the majority of the heat balances for all points run during these tests was 93 percent or greater.

As shown in the figure, the majority of the energy losses are contained in the exhaust losses and the cycle heat rejection to the cooling water. The cycle heat rejection was found by measuring the heat flow to the water passing through the coolers and subtracting off the conduction losses. The total energy flow to the water system also includes the heat losses to the buffer space cooling water and nozzle cooling water which are separate systems from the water flow through the coolers. The heat loss to the exhaust was substantial for these tests due to the high air-fuel ratio maintained (about 40/1 for the points shown). This also tended to have an adverse effect on the overall engine efficiencies measured in these runs.

For any given heater temperature, the conduction losses through the engine are approximately constant. Also, the radiation and convection losses and the nozzle water losses tend to increase much more slowly with pressure than does the heat input from the fuel. Consequently, these losses account for a greater percentage of the heat input at lower pressure levels where the engine output is low. The bargraphs indicate this as the percentage loss due to conduction, radiation and convection, and nozzle water losses at 400 psi is almost double that at 1000 psi. Also, the heat to the buffer water gives some indication of the mechanical losses due to seal friction in the engine. The graphs show that for a constant speed these losses, too, are a much larger percentage of the heat input at the lower pressure and are especially significant when compared to the engine output.

Comparisons of the measured engine output with hydrogen to that predicted by the NASA-LeRC computer simulation are shown in figure 7. The mean compression-space pressure is 300 psi and the heater gas temperature is 1300° F.

The inputs to the computer program were the measured values of heater and cylinder metal temperatures, inlet water temperature and flow rate, engine speed, mean compression-space pressure, and engine temperature profiles for conduction calculations. The mechanical losses were estimated from General Motors GPU motoring and engine performance data given in reference 3.

The curves indicate that the predicted engine output is at most 14 percent higher than the experimental values for each of the four points shown. The brake efficiency comparison which is not shown does not agree as well, being at most 42 percent higher than the experimental values. The efficiency used for the comparison is defined as the brake power divided by the heat into the engine (excludes burner losses). The BSFC values shown in the previous data are based on the measured fuel flow.

The points given in this and the following figure represent the initial direct comparisons between the predicted values and the experimental data. Comparisons to the remainder of the data are now proceeding and will be used to help determine the primary reasons for the differences between prediction and experiment.

Figure 8 shows comparisons of the measured engine output with helium to that predicted by the NASA-LeRC computer simulation. A complete curve is shown for a mean compression-space pressure of 400 psi and a heater gas temperature of 1300° F. Also, two points are shown at 600 psi for the same heater gas temperature.

The predicted engine output is within ± 7 percent of the experimental values at 400 psi and is at most 22 percent higher at 600 psi. Predicted brake efficiency was at most 25 percent higher than the experimental data.

SUMMARY OF RESULTS

The GPU 3 Stirling engine has been converted to a research configuration. The engine was mapped over a limited range at heater gas temperatures from 1100 to 1300° F, mean compression-space pressures from 200 to 1000 psi, and engine speeds from 1000 to 3500 rpm with both hydrogen and helium as the working fluids. The following list is a summary of the major results from these tests.

1. The maximum power obtained with hydrogen was 6.0 hp at 600 psi mean compression-space pressure and 1300° F heater gas temperature. The minimum BSFC was 0.81 lb/hp-hr.

2. The maximum power obtained with helium was 5.25 hp at 1000 psi mean compression-space pressure and 1200° F heater gas temperature. The minimum BSFC was 0.99 lb/hp-hr.

3. Both engine output and efficiency increased with increasing pressure level. However, the relative gain in power and, particularly, the relative gain in efficiency decreased as pressure increased.

4. The maximum efficiency (minimum BSFC) for a given pressure level was obtained at intermediate speeds with flow losses causing the efficiency to decrease at high speeds and conduction losses causing a decrease at the low speeds.

5. The hydrogen power curves were more linear with speed than were the corresponding helium curves giving an indication of the lower flow losses associated with hydrogen.

6. Initial comparisons between the NASA-LeRC simulation predictions and the test data showed that the predicted engine output was at most 14 percent higher than experimental values for hydrogen and at most 22 percent higher than experimental values for helium.

CONCLUDING REMARKS

The NASA-LeRC computer model modification and validation with the data is now underway. These comparisons will be used to help determine the primary reasons for the differences between prediction and experiment. The detailed data will be published along with the engine dimensions necessary for developing similar computer simulations.

Following completion of the tests described in this report, the alternator test setup was removed and replaced with a dynamometer facility. This will allow completion of the mapping over the full engine output range and also provide motoring capabilities to verify mechanical losses.

REFERENCES

1. Cairelli, J. E.; Thieme, L. G.; and Walter, R. J.: Initial Test Results with a Single-Cylinder Rhombic-Drive Stirling Engine. DOE/NASA/1040-78/1, NASA TM-78919, 1978.

2. Tew, Roy; Jeffries, Kent; and Miao, David: A Stirling Engine Computer Model for Performance Calculations. DOE/NASA/1011-78/24, NASA TM-78884, 1978.

3. A Collection of Stirling Engine Reports from General Motors Research, 1958-1970. Vol. 6: Regenerators. GMR-2690-Pt. 6, General Motors Research Labs., Apr. 1978.

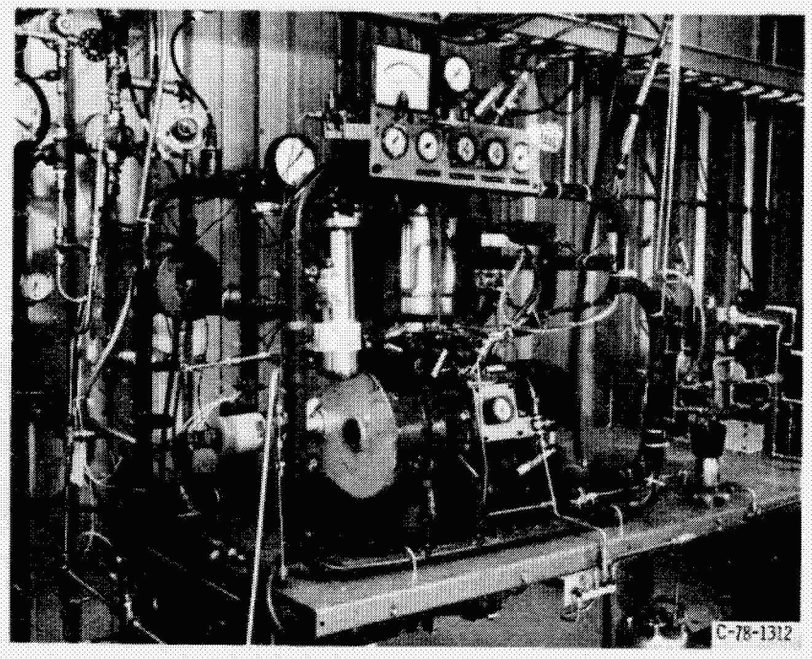

Figure 1. - GPU-3 Stirling engine.

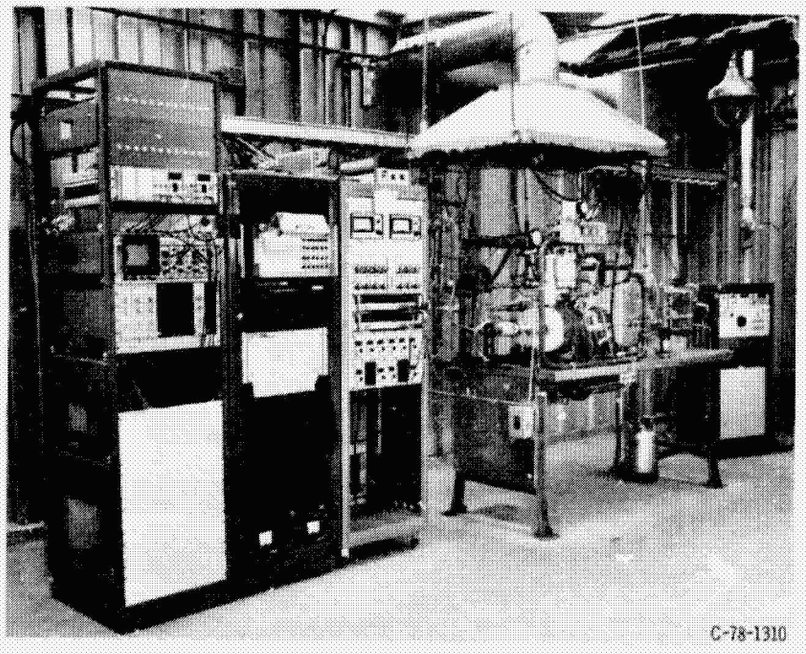

Figure 2. - GPU-3 test setup.

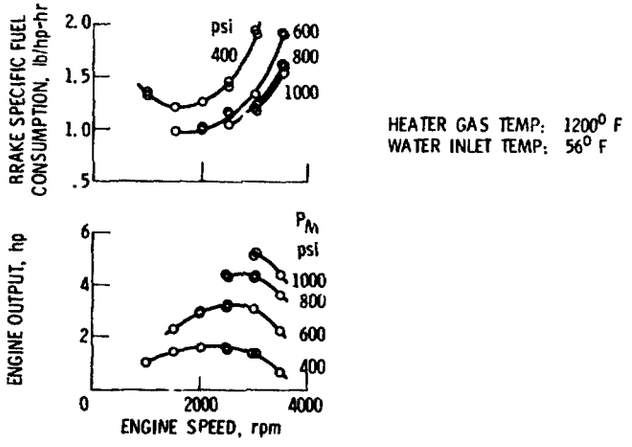

Figure 3. - Helium engine performance as function of engine speed and mean compression-space pressure (P_M).

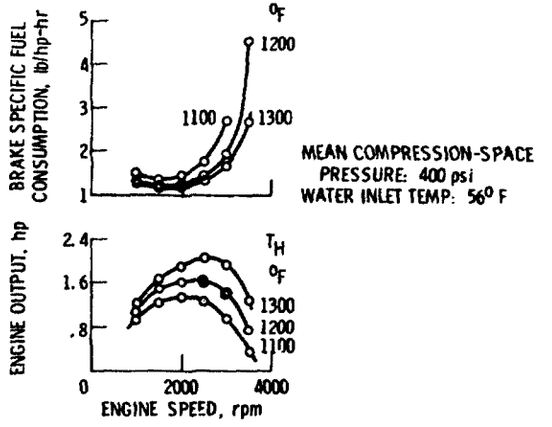

Figure 4. - Helium engine performance as function of engine speed and heater gas temperature (T_H).

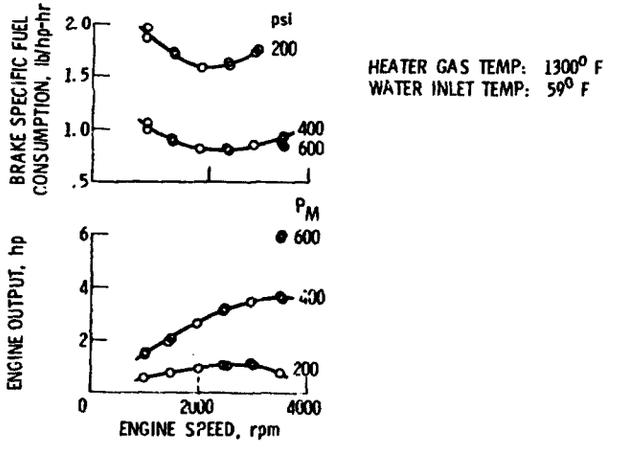

Figure 5. - Hydrogen engine performance as function of engine speed and mean compression-space pressure (P_M).

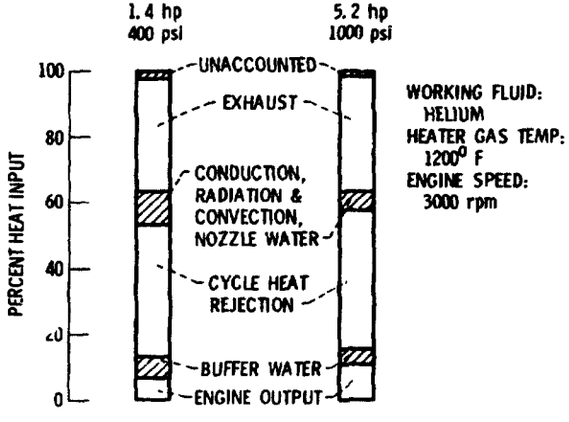

Figure 6. - Energy balances for two mean compression-space pressures.

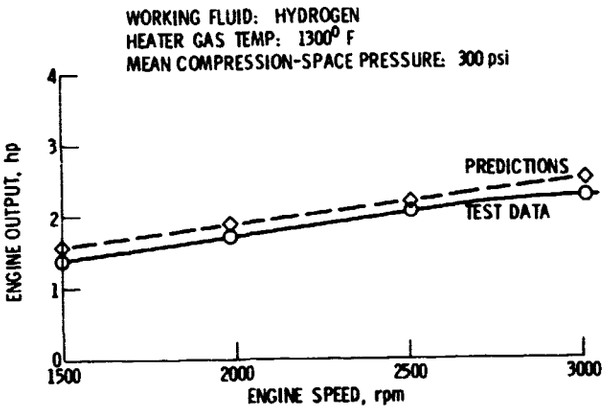

Figure 7. - Comparison of predictions to test data.

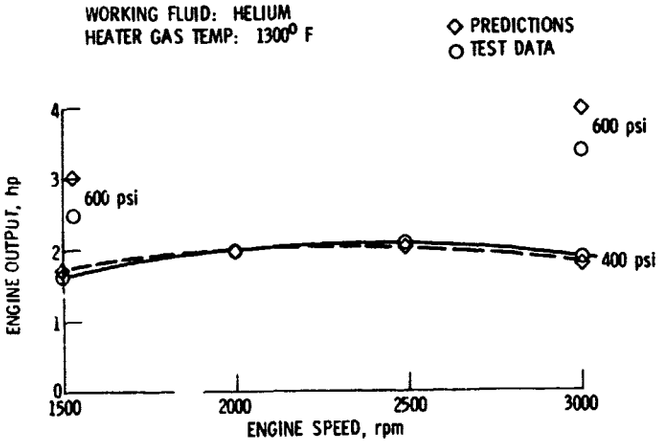

Figure 8. - Comparison of predictions to test data at two mean compression-space pressures.